IEEE Transactions on Nuclear Science, Vol. NS-32, No. 5, October 1985

TRANSVERSE INSTABILITIES DUE TO BEAM-TRAPPED IONS AND CHARGED MATTER IN THE CERN ANTIPROTON ACCUMULATOR

E. Jones, F. Pedersen, A. Poncet, S. van der Meer, E.J.N. Wilson
CERN, CH-1211 Geneva 23, Switzerland

Introduction

At stack intensities above 10^{11} antiprotons with transverse emittances of between π and 2π mm.mrad at 3.5 GeV/c, three distinct transverse heating mechanisms caused by positive matter trapped in the negative beam potential have been observed and identified. Two effects are incoherent and one is coherent. The incoherent effects are of two kinds distinguishable by the rate at which emittance growth occurs, and by the sensitivity to tune changes. The first is a slow growth at a rate which is about equal to, or up to ten times faster than the intrabeam scattering growth rate at small emittances: this is attributed to the excitation of 11th and 15th order non-linear resonances by residual ion pockets, an effect very similar to the beam-beam effect in colliders. The second kind of incoherent effect is an intermittent, violent emittance growth, often associated with a substantial stack loss rate. This effect is believed to be due to multiple Coulomb scattering by highly charged tiny dust particles trapped in the beam potential. Observations of the coherent instability fit the known antiproton-ion (similar to proton-electron) theory. It leads to growth rates faster than the transverse damper presently installed in the AA can handle.

Observation of Abnormal Emittance Growth

The injected antiprotons, initially filling the machine aperture of 90π mm.mrad by 90π mm.mrad, are cooled in momentum, vertically and horizontally by the 1-2 GHz stack core stochastic cooling systems when they are pushed near the stack core orbit[1].

Typical equilibrium core emittances, as measured on a proton stack of $2 \cdot 10^{11}$ p's, are $E_V < 1\pi$ mm.mrad and $E_H = 2\pi$ mm.mrad (95%). This is a balance between cooling rates and intrabeam scattering[2]. With antiproton stacks, above $2 \cdot 10^{11}$, the emittances are often much higher in an unpredictable fashion.

Non-destructive measurements of core emittances are obtained from Schottky scans acquired near 80 MHz by a computer controlled spectrum analyser (Fig. 1). Emittances, tunes and density versus momentum are obtained by unfolding five acquired spectra[3]. In addition, a continuous but less detailed monitoring of core emittances was added to observe their detailed time evolution. Two spectrum analysers operating as fixed tuned receivers are connected to a chart recorder which thus records the total power in a betatron sideband, on a logarithmic scale. This power is proportional to emittance times intensity.

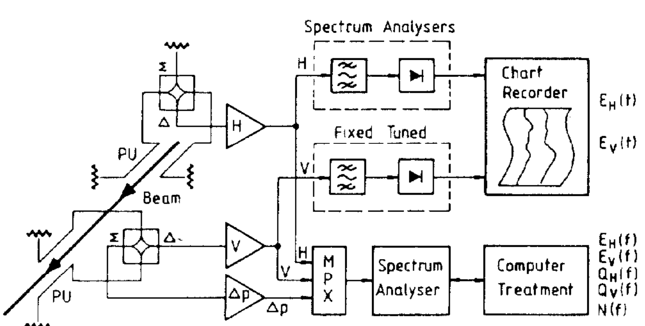

Fig. 1 - Emittance measurements from Schottky noise.

Production, Accumulation and Clearing of Ions

Observations at the AA of ion production from the residual gas and subsequent trapping in the circulating beam consists essentially of two types of measurement: recording of the clearing current on a clearing electrode placed in the middle of one of the two long straight sections with zero dispersion and tune shift measurements with the clearing electrodes turned on or off.

The normal vacuum situation is such that with an average gauge pressure of $5 \cdot 10^{-11}$ Torr with 90% H_2 and 10% of mass 28 (CO or N_2), it takes about 25 s for an antiproton to produce an ion, with roughly equal probability for it to be H_2^+ or CO^+ (or N_2^+).

The natural clearing of ions by Coulomb scattering with the beam is so slow that the ions will continue to accumulate until an equilibrium neutralization of $\eta = 0.998$ (calculated) is obtained. The measured incoherent tune shifts (typ. $\Delta Q_H = +0.003$, $\Delta Q_V = +0.004$ for $N = 2 \cdot 10^{11}$) are compatible with this neutralization.

The AA vacuum chambers were made smooth to avoid neutralization pockets, and many ion collection electrodes were installed, especially at edges of magnets where drift velocities are small. There are 30 clearing electrodes divided in two sets: 12 polarized beam position pick-ups and 18 plates placed in chamber transitions. Inevitably, chamber enlargements due to bellows, special tanks and ceramics exist and create negative potential well pockets of the order of a few volts into which ions are trapped.

During the neutralization process in these pockets[4], ions with high atomic number gain escape energy through multiple Coulomb scattering faster than light ones and are progressively replaced by light species, mainly protons obtained from double ionization of the main residual gas component: H_2.

Non-Linear Resonances Induced by Ion Pockets

The AA magnets are shimmed in such a way that the tune versus momentum is located within the triangle formed by the lines $4Q_V = 9$, $11Q_H = 25$, and the coupling line $Q_H - Q_V = 0$ (Fig. 2). The core tune is located in a region of 15th order resonances. These have so far been ignored since they are not significantly excited by magnet imperfections. However, at antiproton

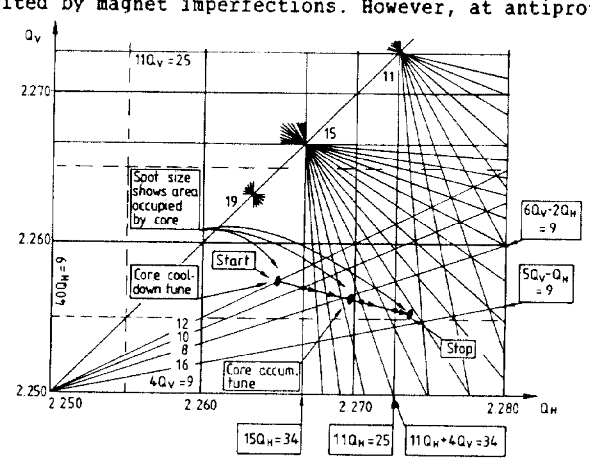

Fig. 3 - Tune diagram with scan line.

stack intensities above 2 × 10^{11} an abnormally high heating rate in the horizontal plane was measured.

Emittances of an intense (N = 2.7 × 10^{11} $\bar{p}$'s) antiproton stack were recorded during a slow horizontal tune scan consisting of 40 steps of ΔQ_H = 0.0002 every 3 min (Fig. 2). Emittance growth due to the crossing of several 15th and 11th order resonances was observed. The net resonance induced heating rates (corrected for cooling and intrabeam scattering rates) are plotted in Fig. 3. One 11th order and two 15th order resonances

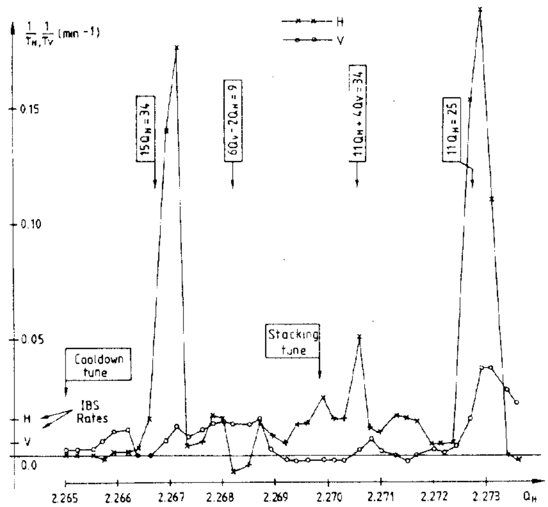

Fig. 3 - Net resonance induced emittance heating rates versus tune.

are seen distinctly, while a generalized heating is observed in the whole area of the 15th order resonances. Also the crossing of an 8th order coupling resonance ($6Q_V$ - $2Q_H$ = 9) is seen as horizontal cooling (E_H > E_V).

An identical tune scan was done with a proton stack of the same intensity, and inverted magnet and clearing polarity. Two resonances were seen, but both were an order of magnitude weaker than with antiprotons.

The resonances observed with antiprotons are thought to be due to excitation by the highly non-linear fields from residual ion pockets while the much faster clearing of electrons by Coulomb scattering explains why the resonances are so much weaker for a proton stack.

The effect is similar to the excitation of non-linear resonances by the beam-beam interaction in colliding beam machines[5]. The electrostatic field of the ion cloud causes non-linear detuning and its uneven distribution excites high order resonances. Another necessary ingredient to explain the growth is some tune modulation which, in the AA, is caused by magnet ripple. The estimated tune modulation amplitude is about ΔQ_{pp} ≈ 3 × 10^{-5} at 300 Hz. Since this is smaller than the stack core tune spread (ΔQ_H ≈ 2 × 10^{-4}, ΔQ_V ≈ 4 × 10^{-4}) only a fraction of the stack is swept across the resonance and heated, but at a faster rate than measured above. This is also evident from the evolution of Schottky betatron sidebands at 1.5 GHz when near a resonance (see Fig. 4). Calculations[6] assuming an average residual neutralization of 10% give growth rates comparable to the measured ones.

Due to the large aperture margin these resonances do not cause losses from the core. However, they are also seen by particles in the stack tail, which basically fill the vacuum chamber, and can cause losses from the tail, effectively reducing the stacking rate. With clearing off, an ion-induced resonance in the tail reduces the stacking rate by 50%. The 15th order resonances have been avoided during cooldown prior to transfer by lowering Q_H to 2.265. However, during accumulation this tune is too close to the coupling line.

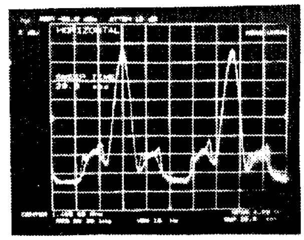

Fig. 4 - Schottky sidebands after 3 min near 11 Q_H = 25.

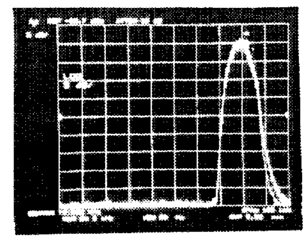

Fig. 5 - Momentum distribution with low energy HF tail.

Effects of Charged Microparticles Captured in the Beam

The sudden onset of an intermittent and often violent emittance growth (τ ≈ 1 min to 1 h), not accompanied by coherent signals is often observed. The abnormal growth sometimes disappears suddenly after a few minutes (Fig. 6); sometimes it tapers off; and sometimes the heating remains for as long as 6 hours preventing any transfers due to high core emittances.

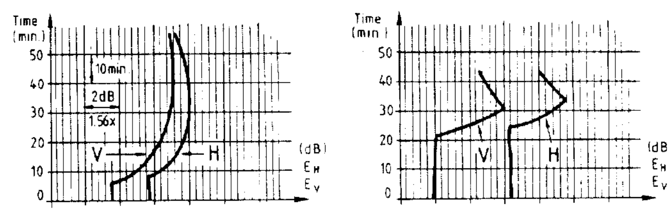

Fig. 6 - Sudden emittance growth from captured, charged microparticle.

There is an associated loss rate, which is typically 10^9/h to 10^{10}/h. A very thinly populated low energy tail (10^{-3} to 10^{-4} times core density) is seen in the momentum distribution (Fig. 5). On the other hand, even after a long time, the mean stack energy loss is below the available spectral resolution of 10 Hz or 200 keV. Occasionally, the onset coincides with an accidental trip of the shutter servos, an event which is known to provoke a mechanical shock in the vacuum chamber. This spooky phenomenon has been dubbed the AA "Ghost". All its characteristics observed so far can be explained by the effects of a tiny, highly positively charged microparticle captured in the beam potential[7]. Although the material is not precisely known (and probably differs from case to case), typical calculated parameters are shown in Table 1. A possible material should have fairly low density, be strong, hard to sublimate, have a high melting point, and a low work function.

The scattering occurs predominantly in the external electric field. If the observed emittance growth were to be explained by multiple scattering on nuclei alone, the amount of matter involved would cause an observable energy shift and a much higher loss rate.

The particle is positively charged by close antiproton-electron Coulomb collisions knocking off secondary electrons of sufficient energy to escape the particle potential, and the low energy tail consists of those antiprotons that have suffered a large energy loss from these collisions. Three possible discharge mechanisms exist, namely: 1) collection of low energy secondary electrons from beam-gas interactions, 2) field ionization[8] of the residual gas (above ~20 GeV/m for H_2), and 3) field evaporation[8] of ions of the particle material. At low beam densities the residual

Table I

Typical Microparticle Parameters $N = 2 \times 10^{11}$ $\epsilon_H = 3\pi$ mm.mrad $\epsilon_V = 1.5\pi$ mm.mrad	
Material	SiO_2
Radius	1 µm
Power dissipation	4.2 µW
Temperature	1556°K
Surface field	52.4 GV/m
Voltage	52.4 kV
Charge	3.6×10^7 e
Surface tension	1242 kg/mm²
Multiple Coulomb scattering on nuclei	$\{\tau_H = 114$ min, $\tau_V = 46$ min
Multiple Coulomb scattering in ext. field	$\{\tau_H = 2.8$ min, $\tau_V = 1.1$ min
Loss rate	1.4×10^9/h
Stack freq. shift rate,	$\dot{f} = 0.48$ Hz/min
Transverse oscillation frequencies	$\{f_H = 3.0$ kHz, $f_V = 3.3$ kHz
Drag force	1.38×10^{-14} N
Acceleration (if free)	1.49 m/s²
Required stop field	2.4 mV/m

gas electron current dominates, and at typical AA beam densities, the surface field is limited by the field evaporation threshold. The field ionization current never dominates.

The extreme mechanical stress in Table I is not impossible. Stresses 80 times the technical tensile strength have been reported in field ion microscopes[9].

Charged microparticles may be successfully eliminated from the beam by cycling the clearing fields. When the clearing is switched off, the beam potential is reduced by almost 3 orders of magnitude, and the reduced longitudinal field component lets the particle move along the lattice under the combined influence of the beam drag force and residual kinetic energy. Changes in emittance growth rates and loss rate are often observed. When the clearing field is switched back on, the particle is more often than not removed from its new position, and the heating disappears.

Coherent Antiproton-Ion Instabilities

Coherent instabilities on the lowest transverse dipole mode (baptised hiccup) leading to beam growth of dense cooled stacks have been identified in the AA. These instabilities limit the minimum vertical emittance to a value proportional to intensity for stacks of more than typically 2×10^{11} $\bar{p}$'s. The same is true in the horizontal plane above 3.1×10^{11} $\bar{p}$'s.

Protons in the beam potential wells of the AA long straight sections are thought to be responsible for these instabilities. Their coherent bounce frequencies in the antiproton potential well (1200-1500 kHz) correspond to the lowest unstable transverse dipole mode of the beam $(3 - Q)f_{rev}$. The process is identical to the electron proton instability already seen in the ISR[10-11].

One hiccup lasts typically 1 minute during which the emittance increases by 10%. It consists of several (5 to 10) microinstabilities with 10 ms e-folding growth time, each increasing the emittance by ~1% stepwise, until the neutralization threshold with ions of lower frequencies cannot be reached any more. The cooling system then reduces the beam size to the initial threshold and the same process starts again (Fig. 7. Figure 8 shows a spectrum analyser photograph of the coherent signal.The present transverse damper system does not provide enough gain in the frequency range concerned to control the instability.

As the instability is also a clearing mechanism the flow of ions to the nearby clearing electrode is momentarily diminished (Fig. 7).

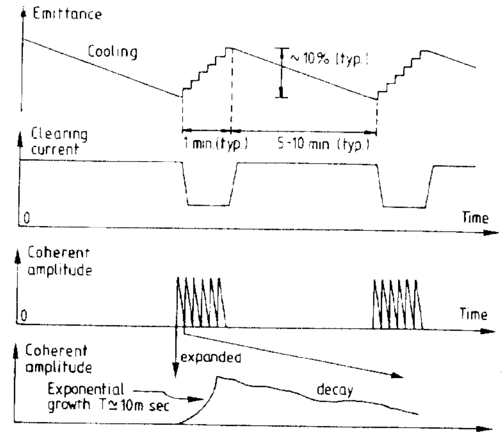

Fig. 7 - Coherent antiproton-ion instability.

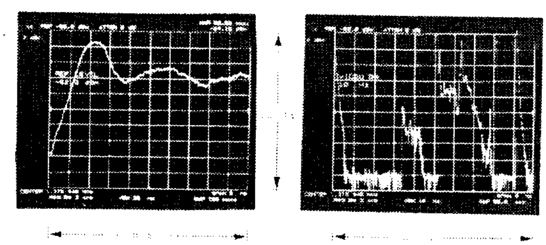

Fig. 8 - Amplitude of lowest vertical betatron line $0.74 * f_{rev}$.

Conclusion and Cures

All three effects mentioned are potential limitations to the CERN antiproton accumulator performance, in particular at the higher stack intensities expected after completion of the ACOL[13] project in 1987 and remedies are under way. These consist of further elimination of residual potential well pockets by installing additional clearing electrodes, and reshimming of magnets to avoid ion-induced resonances. The damper will also be improved to have sufficient gain to handle coherent instability.

References

[1] S. van der Meer, IEEE Trans. Nucl. Sci., Vol. NS-28, p. 1994, 1981.

[2] M. Martini, CERN PS/84-9 (AA), 1984.

[3] S. van der Meer, PS/AA/Note 84-11, 1984.

[4] A. Poncet, PS/AA/ME/Note 81, 1985.

[5] L. Evans, CERN SPS/83-38, 1983.

[6] E.J.N. Wilson, Private Communication.

[7] F. Pedersen, Report to be published.

[8] E.W. Müller, Advances in Electronics and Electron Physics, Vol. 13, p. 83, 1960.

[9] E.W. Müller, Journal of Applied Physics, Vol. 38, p. 2070, 1967.

[10] H.G. Hereward, CERN 71-15, 1971.

[11] E. Keil and B. Zotter, ISR-TH/71-58, 1971.

[12] F. Pedersen, W. Pirkl and K. Schindl, IEEE Trans. Nucl. Sci., Vol. NS-30, 2343, 1983.

[13] E.J.N. Wilson, CERN 83-10, 1983.